



# Increasing heavy rainfall events and associated excessive soil water threaten a protein-source legume in dry environments of West Africa

Toshichika Iizumi<sup>a,\*</sup>, Kohtaro Iseki<sup>b</sup>, Kenta Ikazaki<sup>b</sup>, Toru Sakai<sup>b</sup>, Hideo Shiogama<sup>c</sup>, Yukiko Imada<sup>d</sup>, Benoit Joseph Batieno<sup>e</sup>

<sup>a</sup> National Agriculture and Food Research Organization (NARO), 3-1-3 Kannondai, Tsukuba, Ibaraki 305-8604, Japan

<sup>b</sup> Japan International Research Center for Agricultural Sciences (JIRCAS), 1-1 Ohwashi, Tsukuba, Ibaraki 3058-686, Japan

<sup>c</sup> National Institute for Environmental Studies, 19-2 Onogawa, Tsukuba, Ibaraki 305-8506 Japan

<sup>d</sup> Atmosphere and Ocean Research Institute, The University of Tokyo, 5-1-5 Kashiwanoha, Kashiwa, Chiba 277-8564, Japan

<sup>e</sup> Institut de l'Environnement et de Recherches Agricoles (INERA), Station de Kamboinse B.P. 476, Ouagadougou, Burkina Faso

## ARTICLE INFO

### Keywords:

Climate change  
Cowpea  
Crop model  
Heavy rainfall  
Nutrition  
Soil

## ABSTRACT

The intensification of the hydrological cycle has increased heavy rainfall and drought events in a changing climate. However, compared to drought, the impacts of heavy rainfall on crop production are under-studied. Using field experimental data and a calibrated crop model CYGMA, we showed that excessive soil water associated with heavy rainfall events is having a detrimental effect on cowpea yields, even in the dry environments of West Africa where cowpea is an important, protein-rich cash crop. Cowpea yields are susceptible to heavy rainfall in areas with poorly drained soils, and to drought in soils that have a low water-retention capacity. The crop model captured the main characteristics of the observed development, growth, and yield, as well as the characteristics of root-zone soil water contents and how they vary by soil type. The analysis of d4PDF factual and counterfactual climate model simulations revealed that heavy rainfall events associated with anthropogenic climate change have increased in recent decades, and that they are projected to increase in future. Further, changes in seasonal rainfall and the number of dry days would be largely absent from CMIP6 climate projections by mid-century. Reductions in cowpea yields due to excessive soil water is projected to become more frequent, and the potential damage in a 1-in-100 extremely wet year would be comparable to the damage currently experienced in droughts, irrespective of soil types. Simulations of the projected damage due to drought show that the situation will be similar to current levels, with drought remaining a major climate hazard. However, excessive soil water is projected to be a serious threat to food security in the region. Our findings indicate that, even in dry environments, cropping systems need to be implemented in order to reduce the susceptibility of soils to both drought and excessive soil water.

## 1. Introduction

The intensification of the hydrological cycle in recent decades has increased the risks of both droughts and heavy rainfall events to agriculture (Donat et al. 2016; Vogel et al. 2019). However, compared to droughts, which are a well-documented climatic-impact drivers of production shocks, food price spikes, food insecurity, and social unrest (Brown et al., 2006; Kim et al., 2019; Food and Agriculture Organization, 2021; Anderson et al. 2021), the effects of heavy rainfall on crop production have been under-studied. Heavy rainfall events can decrease crop production through the adverse effects that excessive soil water can

exert on plant physiology (Mitchell et al. 2013; Irmak 2014), even in the absence of physical damage from flooding, such as being dislodged by runoff (Kim et al., 2023).

The few studies have shown that heavy rainfall can have either negative or positive effects on yields. For example, heavy rainfall has been shown to reduce maize yields in cooler regions with poorly drained soils by 17 %, compared to normal yields based on long-term trends (Li et al., 2019); such a decrease is considerable compared to yield reduction due to drought (32 %). A pioneering study by Rosenzweig et al. (2002) showed that, by the 2030s, the frequency of heavy rainfall events in the US might be twice that of 1951–1998 levels, and that crop

\* Corresponding author.

E-mail address: [iizumit@affrc.go.jp](mailto:iizumit@affrc.go.jp) (T. Iizumi).

<https://doi.org/10.1016/j.agrformet.2023.109783>

Received 21 December 2022; Received in revised form 4 October 2023; Accepted 22 October 2023

Available online 20 November 2023

0168-1923/© 2023 The Authors. Published by Elsevier B.V. This is an open access article under the CC BY-NC-ND license (<http://creativecommons.org/licenses/by-nc-nd/4.0/>).

production losses due to excess soil water may amount to \$3 billion per year. Attributing the effect of heavy rainfall on decreasing crop yields to climate change has been challenging (Urban et al. 2015), and researchers have only recently begun to consider this effect in climate change impact assessments. In a recent assessment using a multi-crop model ensemble, some of the models showed that the negative impacts of excessive soil water on yields in humid regions of the world could offset increases in yields due to the fertilization effect of elevated atmospheric carbon dioxide concentrations [CO<sub>2</sub>] (Jägermeyr et al. 2021).

The negative impacts of excessive soil water have also been reported for legume crops cultivated in dry regions of West Africa where water-logging due to heavy rainfall in conjunction with high soil temperature restrict root nodulation and decrease yields (Iseki et al., 2021). Given the already fragile status of agricultural production and food insecurity in the region, the potential impacts of excessive soil water in a changing climate need to be better understood within the context of climate-resilient development.

Cowpea (*Vigna unguiculata*) is a legume crop that is widely grown in West African Sudan Savanna (Callo-Concha et al. 2013). The average rainfall from mid-July to mid-October ranges from 300 to 1000 mm [Fig. S1, Fig. S2]. Over 7.6 million metric tons of dried cowpeas (i.e., 86 % of global production in 2020) is produced in the region (Food and Agriculture Organization FAO, 2022). Cowpeas are produced by farmers with an average field size of <2 ha to 5–15 ha (Samberg et al., 2016). Farmers in the region cultivate cowpea using either a mixed-cropping system with sorghum, a major staple crop, or as the sole crop for self-consumption, to produce hay for livestock, or to generate cash (Shiratori et al., 2020; Smale and Thériault 2021). Considering that the population of West African countries was 403 million in 2020 (United Nations, 2022), the average amount of per capita annual cowpea consumption is 19 kg. Since cowpea contains 25 % protein (Vasconcelos et al. 2010), the daily protein intake is 13 g, which is approximately a quarter of the recommended daily allowance for a sedentary adult (i.e., 46–56 g depending on body weight) (National Academies of Sciences, Engineering, and Medicine 2005).

Despite the importance of cowpea for nutrition and for generating income, yields vary markedly in different locations due to differences in rainfall patterns, varieties, and soil types. Soil nutrient deficiencies (in particular, phosphorous) are also known to be a limiting factor for legume yields (Sanginga et al., 2000; van Heerwaarden et al. 2023). In West Africa, soils vary, with the main types being lixisols (LX) and plinthosols (PT) (Fig. S2). Moreover, at a local scale, these soil distribution patterns depend on the distance from river channels (LX tend to be distributed on the lower to toe slopes, while PT soils tend to be distributed on the middle to upper slopes). These soils also differ markedly in terms of rooting depth (LX, 75 cm and PT, 25–50 cm), nutrient contents, and water-holding capacity; these factors lead to differences in average crop yields between these soil types (Ikazaki et al., 2018; Iseki et al., 2021). Interactions between genotypes and the environment also affect yield responses to soil water deficits and excessive soil water (Padi and Ehlers 2008; Iseki et al., 2021), and make it difficult to simultaneously increase yields under favorable growing conditions and maintain yields under stressed conditions (Padi 2004). For example, the coefficient of variation for cowpea yield in Burkina Faso is 29 % (Fig. S3), which implies that stable cowpea production has not yet been achieved in the region and will be even more challenging in the face of climate change.

Although drying of the surface soil has been observed in West Africa from the 1950s to the present, the confidence associated with projections of future rainfall are low, with drying projected in the western parts of the region and wetting in the eastern parts of the region (Arias et al. 2021). West Africa, especially in the east, is economically, socially, and infrastructurally vulnerable to droughts (Carrão et al., 2016), and probably to heavy rainfalls as well. Here, we provide evidence showing the adverse effect of heavy rainfall on cowpea yields, even in the dry

areas of the West African Sudan Savanna. Using a process-based crop model that considers cowpea varieties that are tolerant to excessive soil water and deficits in soil water, we also present a comparison of yield impacts due to excessive soil water from heavy rainfall and the impacts on yield due to drought in the middle of this century.

## 2. Materials and methods

Field experiment data were obtained for 20 varieties and three soil types in four growing seasons (2016–2019). These data were used to estimate the average cross-variety yield responses to rainfall patterns and soil dependence. A process-based crop model was calibrated for each soil type using the calibration subset of the field experiment data (2016 and 2019). The performance of the model was evaluated against all data. Then, the model was used to simulate the rainfed cowpea yields for each variety and soil type over the current (1990–2019) and near-future (2020–2049) periods using CMIP6 climate projections. In addition, an analysis of two different sources of climate information (d4PDF and CMIP6) was performed to assess the consistency of climate-model-simulated changes in cowpea-season rainfall characteristics between factual and non-warming counterfactual climate conditions (d4PDF), and among the preindustrial, recent, and near-future periods (CMIP6). See Texts S1 and S2 in Supplementary material for CMIP6 and d4PDF climate data, respectively.

### 2.1. Field experiment data

Data were obtained from field experiments conducted at the Institute of Environment and Agricultural Research (INERA)'s Saria experimental station in Burkina Faso (12.27°N, 2.15°W, 300 m above sea level). The varieties considered here comprised 14 landraces [seven each, from the southern (ID 02, 05–10) and northern regions (ID 03, 04, 11–15) of Burkina Faso] and six breeding lines (ID 01, 16, 18, and 20 from Burkina Faso, ID17 from Nigeria, and ID 19 from Senegal) (Table S1). Sixteen of these varieties were described in Iseki et al. (2021). The data were collected for four seasons from 2016 to 2019, three soil types [Ferric Lixisols (LXfr), Petric Plinthosols (PTpt), and Pisoplinthic Petric Plinthosols (PTpt.px)], two nitrogen (N) fertilizer treatments (0 and 14 kg N ha<sup>-1</sup> yr<sup>-1</sup>), two planting densities (3.13 and 6.25 plants m<sup>-2</sup>), and five replicates. The data recorded include 1440 samples (n). The items recorded include dates of sowing, flowering, and harvesting, extent of canopy cover, leaf area index (LAI), above- and below-ground biomass, and grain yield. The canopy cover is the proportion of the land area that is covered by the crop canopy. The canopy cover, LAI, and biomass were measured multiple times during each season.

### 2.2. Local weather observations

We used daily weather observations for the period 2016–2019 obtained from the experimental station. The data included the daily mean, maximum, and minimum air temperatures, precipitation, solar radiation, relative humidity, and wind speed. Missing values only accounted for a small fraction of the data (2 % in 2016). We also measured daily soil water content for each soil type from July 24, 2016 to December 27, 2019 in the cowpea fields. Cultivation was performed using ID 01, no N fertilizer input, and sowing performed on day of year (DOY) 199 to 208. Measurements were taken in multiple soil layers (LXfr, four layers at 0–75 cm deep; PTpt, three layers at 0–50 cm deep; and PTpt.px, two layers at 0–25 cm deep) and aggregated to derive the root-zone soil water content for each soil type with different rooting depths (LXfr, 75 cm; PTpt, 50 cm; and PTpt.px, 25 cm). Additional information on the data collected is described in Iseki et al. (2021).

### 2.3. Yield responses to rainfall patterns

To derive cross-variety average responses to rainfall patterns, we first

calculated the average yield for each N fertilizer level and soil type using all data. We then computed the relative yields against the average. The yield response in the LXfr soil type (referred to as LX for simplicity;  $n = 64$ ) was compared to the yield response in PTpt and PTpt.px soil types after these two were combined as one group (referred to as PT;  $n = 124$ ). These types are similar in terms of hydrological characteristics than either is to LXfr. To visualize cross-variety responses of average relative yield to rainfall patterns, locally weighted scatterplot smoothing (LOWESS; Cleveland 1979) curves were plotted using the statistical package R, version 4.1.1 (R Core Team 2021). High- and low-yielding varieties were identified for LX and PT soils based on average relative yield over the years.

## 2.4. Crop model

### 2.4.1. Overview

The global gridded crop model CYGMA (the Crop Yield Growth Model with Assumptions on climate and socioeconomics) was used. Although the model was originally designed for climate risk assessment at a global scale (Iizumi et al. 2017; Iizumi et al. 2018; Jägermeyr et al. 2021), it has been applied to national- and regional-scale analyses (Sultan et al., 2019; Iizumi et al. 2021a; Iizumi et al. 2021b; Ishikawa et al., 2021).

The model has a  $0.5^\circ$  resolution and employs daily time steps. We only considered rainfed conditions in this study. Crop development is calculated as a fraction of the accumulated growing degree days relative to the crop total thermal requirements. Leaf area expansion and senescence are calculated based on the fraction of the growing season under the prescribed shape of the LAI curve. Yields are calculated using the photosynthetically active radiation intercepted by the crop canopy, the radiation-use efficiency (RUE), the fertilization effect on RUE from elevated  $[\text{CO}_2]$ , and the fraction of biomass increase allocated to the harvestable component. The effect of stomatal closure on actual evapotranspiration under elevated  $[\text{CO}_2]$  is also considered. The root-zone soil water content is used to calculate the actual evapotranspiration. Descriptions on soil water balance modeling are available in Section 2.4.2.

Five different stress types, i.e., N deficit, heat, coldness, water deficit, and water excess, are considered. The most dominant stress type on a given day decreases the daily potential increase in the LAI if the crop is in the vegetative growth stage, or the yield if the crop is in the reproductive growth stage. Except for N deficit, all of the stress types are functions of daily weather. The N deficit stress is calculated based on the annual N application rate, crop N uptake, and N leaching (Text S3). Although cowpea is a legume that can fix nitrogen, cowpea yields at the experimental station are sensitive to the total amount of soil nitrogen (Iseki et al., 2021). For this reason, we considered N deficit stress, although we have set the sensitivity of cowpea yield to N deficit stress as being considerably less than that of cereals, as was done for soybean in Iizumi et al. (2017). The model's sensitivity to N application rates was determined based on the observed differences in the LAI, above-ground biomass, and grain yield between the two levels of N application rate. The soil water excess stress occurs on days when the root-zone soil water ( $W$ ) is close to saturation. The water deficit stress is calculated using the ratio of the actual and potential evapotranspiration rates. Although heat and cold stresses were considered in the model, they were not focused on in this study. Additional information on modeling the stresses is described in Iizumi et al. (2017).

### 2.4.2. Water excess stress

The water balance in the root zone at day  $t$  over an area is expressed as:

$$\frac{dW}{dt} = P - E - R - G \quad (1)$$

where,  $W$  is the soil water content;  $P$  is precipitation;  $E$  is the actual crop evapotranspiration;  $R$  is the net streamflow divergence; and  $G$  is the net groundwater loss through deep percolation. The unit of these terms is  $\text{mm H}_2\text{O}$ . The streamflow divergence ( $R$ ) consists of surface runoff ( $S$ ) and subsurface runoff (or base flow,  $B$ ):

$$R = S + B \quad (2)$$

According to Huang et al. (1996), the surface and subsurface runoff are parameterized as follows:

$$S = P \left[ \frac{W}{W_{\max}} \right]^m \quad \text{and} \quad B = \frac{\alpha}{1 + \mu} W \quad (3)$$

where,  $W_{\max}$  is the plant-extractable root-zone soil water capacity ( $\text{mm H}_2\text{O}$ );  $m$  is a parameter with values greater than 1 and indicates the increase in surface runoff with soil water saturation;  $\alpha$  is the inverse of the response time of the baseflow, with a larger  $\alpha$  value indicating good drainage capacity of the soil (or poor water retention) (Table S2); and  $\mu$  is a dimensionless parameter that determines the proportion of the subsurface flow that becomes baseflow. The remaining portion is lost as groundwater and is given as follows:

$$G = \frac{\mu\alpha}{1 + \mu} W \quad (4)$$

In reality, although runoff and soil water move laterally and increase the soil water content of neighboring areas or enter river channels or local reservoirs (Neitsch et al., 2005), in the model, surface runoff, subsurface runoff, and groundwater are lost from the root-zone soils to areas outside of the model's system boundary. Consequently,  $W/W_{\max}$  is never greater than 1.

In the model, the calculation of excess water stress is performed after one day with near-saturation condition ( $W/W_{\max} > 0.9$ ), as did conceptually similar in Rosenzweig et al. (2002). The use of  $W/W_{\max} > 0.9$  is based on the observation that cowpea growth retardation due to excessive soil water occurs even when soil water is below field capacity (Iseki et al., 2023). Further, according to modeling of Wang et al. (2016), stress factor values become increasingly severe from partial to full saturation. While the excess soil water stress reduces the daily potential increase in the LAI and yield, it does not affect simulated phenological development. Although inundation, pests, and diseases under wet conditions damage crops, the model only considers low aeration conditions and associated stress for root growth and root N fixation. Since N leaching increases depending on subsurface runoff and baseflow, the N deficit stress increases when heavy rainfall events occur (see Text S3).

## 2.5. Calibration and validation

Cowpea genetic coefficient values were determined based on the field experiment data obtained for two seasons (2016 and 2019) and from the literature. The total crop thermal requirement ( $GDD_c$ ) and the fraction of the growing season when flowering occurs ( $f_{r_{GDD,ant}}$ ) were calculated using the observed crop and daily mean temperature data (Fig. S4). The largest LAI value identified for each variety in the calibration subset was taken as the maximum LAI under optimal conditions ( $LAI_{\max}$ ). The base and maximum temperatures for development, as well as the RUE value, were based on the literature and are commonly used between the different varieties [ $T_b = 9.5^\circ\text{C}$  and  $T_u = 42^\circ\text{C}$  from Craufurd et al. (1997);  $\text{RUE} = 1.64 \text{ g MJ}^{-1}$  from Sousa et al. (2018)]. The RUE value at the elevated  $[\text{CO}_2]$  of 660 ppm was 1.1-times higher than that in the ambient  $[\text{CO}_2]$  according to Neitsch et al. (2005). Finally, we also determined the curvature factor values of the stress functions on soil water excess and deficit ( $\alpha_{W_{\text{exs}}}$  and  $\alpha_{W_{\text{def}}}$  in Iizumi et al. 2017) for each soil type that gave a good match between the modeled and observed LAI, above-ground biomass, and yield. Although the tolerance to these stresses (i.e., the form of the stress functions) may vary among varieties (Bastos et al. 2011), we only considered the difference in drainage

capacity between the soil types due to the limited data.

We also set the model's hydrological properties for each soil type to match the observed soil water content in 2016 and 2019. The soil properties determined for each soil type included the plant-extractable root-zone soil water capacity ( $W_{max}$ ) and the inverse of the response time of the baseflow ( $\alpha$ ) (Table S2). The  $\alpha$  value represents the drainage capacity of soil, as mentioned earlier. We identified the 95th percentile values of the observed maximum root-zone soil water content from the calibration subset and used it as the  $W_{max}$  value. Through trial and error, we searched for an  $\alpha$  value for each soil type that showed a good agreement between the modeled and observed soil water contents.

The model performance was evaluated through a comparison of all data (i.e., both the calibration subset and the remaining subset). To ensure that comparisons were consistent, data processing was performed as follows. As there were fewer LAI values than canopy cover values, the observed canopy cover values were converted into LAI values using an empirical relationship established from the field experiment data [ $LAI=0.073+0.016*\text{canopy cover}$ ;  $n = 815$ ;  $R^2=0.643$ ]. This was done to compare the field observations with the model that outputs LAI, but not canopy cover. Little sample was also available for below-ground biomass. We therefore calculated the average fraction of the above-ground biomass to the total biomass from the data and then multiplied this value by the modeled total biomass to obtain modeled above-ground biomass. Then, season maximum values for LAI and above-ground biomass were used for the comparisons. Since the model considered only average planting density, data obtained from paired observations, in which all other treatments except planting density were the same, were averaged.

### 2.6. Yield projections

We performed yield projections using the calibrated crop model and climate projections using two radiative forcing scenarios, five GCMs (Table S4), and two bias-correction methods (Text S1). As rainfall projections for the near future were not obviously different each other, these radiative forcing scenarios were treated as equivalent futures. To consider the fertilization effect and increased water-use efficiency in the crop model, elevated  $[CO_2]$  corresponding to two scenarios (469 ppm and 563 ppm for 2050 under SSP126 and SSP585, respectively) were used. Sowing dates (DOY 200) were kept the same. A total of 20 cowpea varieties were simulated. No N fertilizer input was assumed. In total, we obtained 72,000 rainfed cowpea yields for the two radiative forcing scenarios, five GCMs, bias-correction methods, three soil types, 20 varieties, and 60 years (1990–2049) over Burkina Faso. The modeled yields in the  $0.5^\circ$  grid cell in which the experimental station is located were extracted and used to derive the empirical cumulative distribution function (CDF) of the modeled yield for dryer- and wetter-than-optimal years. The optimal rainfall was set to 550 mm (Fig. S5 a) since the climate projections were bias-corrected using JCS meteorological forcing data as a reference. The yield value in a 1-in-100 extremely wet year was identified from each of the CDFs for the variety that was most tolerant to excessive soil water (ID 19), as well as the remaining relatively less-tolerant varieties under both the present-day (1990–2019) and near-future (2020–2049) climates. As in the extremely wet year, the yield value in an extremely dry year was identified for the most drought-tolerant variety (ID 12), as well as for other remaining varieties in the present-day and near-future climates. These varieties were selected because the model was able to reproduce the relative tolerance of them qualitatively well (Fig. S6).

## 3. Results

### 3.1. Yield response to soil water excess and deficit

The field experiment data revealed that the optimal seasonal rainfall for cowpea is around 400 mm, above which yield decreased (Fig. 1a).

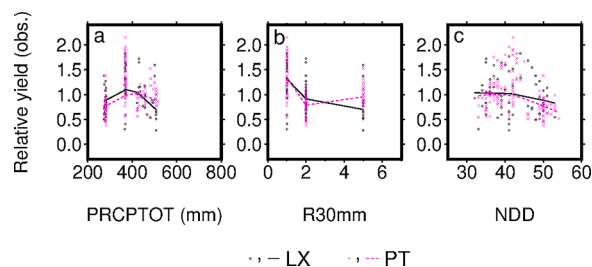


Fig. 1. Observed cowpea yield response to rainfall patterns. Average relative yield of varieties and agronomic treatments following seasonal rainfall (a, PRCPTOT), number of heavy rainfall days (b, R30mm), and number of dry days (c, NDD). Black and magenta lines indicate the average responses for two soil types, LX (ferric lixisols) and PT (petric plinthosols and pisoplinthic petric plinthosols), derived using locally weighted scatterplot smoothing.

The yield response to rainfall patterns varied by soil type. In LX soils with higher water retention (lower drainage potential), yields decrease rapidly as the number of heavy rainfall days [daily precipitation ( $P>30$  mm)] increases (Fig. 1b). In PT soils with lower water retention (higher drainage potential), yields decrease markedly for up to two heavy rainfall days, but many more heavy rainfall days have less influence on yields. When the number of dry days ( $P<1$  mm) increases, yields decrease rapidly in PT soils, while yields decrease only mildly in LX soils (Fig. 1c). The difference in water retention and drainage between the soil types contributes to the contrasting yield responses to dry and wet soils, on a varietal average basis.

Different cowpea varieties respond differently to wet and dry soils. Varieties that perform relatively well in wet soils do not typically perform well in dry soils. Among the 20 cowpea varieties tested in this study, some of the northern landraces from Burkina Faso (ID 12 and ID 14), which mature later and have an intermediate LAI, are more tolerant of dry soils. On the other hand, breeding lines from Senegal (ID 19) and Burkina Faso (ID 20), which mature earlier and have a larger LAI, are more tolerant to wet soils (Fig. 2; Table S1, Fig. S4). The low-yielding varieties were ID 07 in dry soils and ID 08 in wet soils, irrespective of the soil types. Both varieties are from the southern landrace in Burkina Faso and are characterized by having a shorter to intermediate maturity and intermediate to larger LAI.

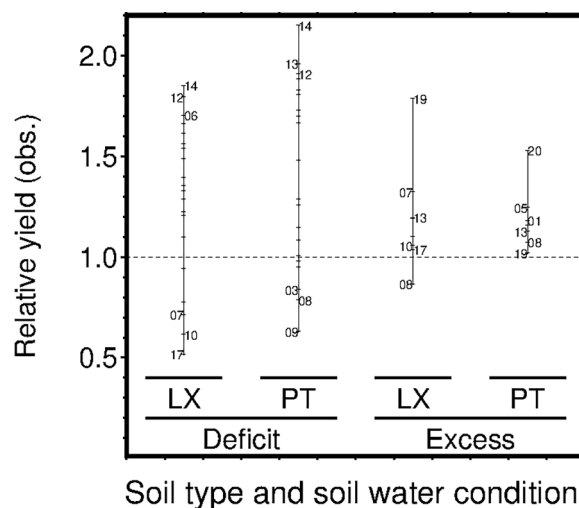


Fig. 2. Different observed varietal responses to soil water excess and deficit. Relative yields of high- and low-yielding varieties (three each) for two soil types, LX (ferric lixisols) and PT (petric plinthosols and pisoplinthic petric plinthosols).

### 3.2. Model representation

#### 3.2.1. Soil water content

The calibrated CYGMA model was able to capture some major characteristics of the observed root-zone soil water content in cowpea fields at the experimental station, irrespective of the soil type. When weather observations are used to drive the model, the Pearson's correlation coefficients ( $r$ ) calculated between the observed daily data and model outputs for four seasons from 2016 to 2019 were all significant at the 1 % level, although the correlations were moderate in absolute terms, i.e.,  $r = 0.219$  (PTpt) to  $0.569$  (PTpt.px) (Fig. 3; Table S3). The root-mean-squared error (RMSE) ranges from 15 % (LXfr) to 27 % (PTpt), relative to the average of the observations.

#### 3.2.2. Development, growth, and yield

Comparisons of the modeled development, growth, and yield with the field experimental data are summarized in Fig. 4. The results show

that the model accurately reproduced the observed dates of flowering (flw) and harvesting (hvt), with  $r$  and RMSE values being  $\geq 0.788$  and  $\leq 1$  %, respectively (Table S3). The modeled growth of the season maximum above-ground biomass (bio) and LAI (lai) had moderate to high  $r$  values of  $\geq 0.305$ , with errors  $\geq 29$  % being larger than those obtained for the modeled flowering and harvesting dates. Season maximum above-ground biomass tended to be overestimated, while no such bias was observed for season maximum LAI. The agreement between the modeled yields and data (yld) was diverse, ranging from a low  $r$  value of  $0.291$  ( $p = 0.011$ ) to a moderate  $r$  value of  $0.556$  ( $p < 0.001$ ) with an RMSE value of  $\leq 54$  %.

#### 3.2.3. Yield response

The yield response to soil water conditions reproduced by the model using JCS meteorological forcing data was qualitatively in good agreement with the observed results, despite being wet-biased in absolute terms. Although the model was able to reproduce the different response

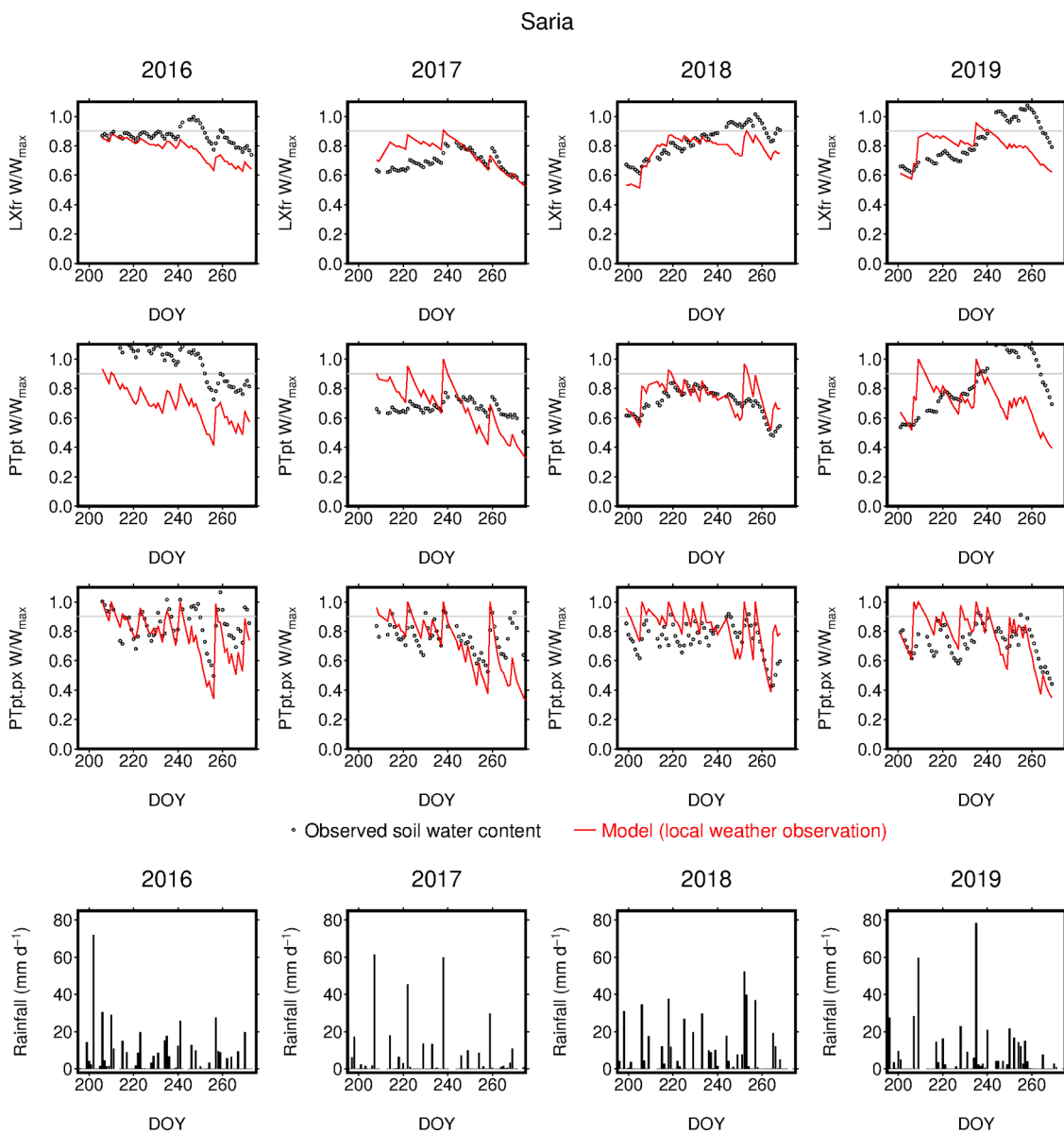
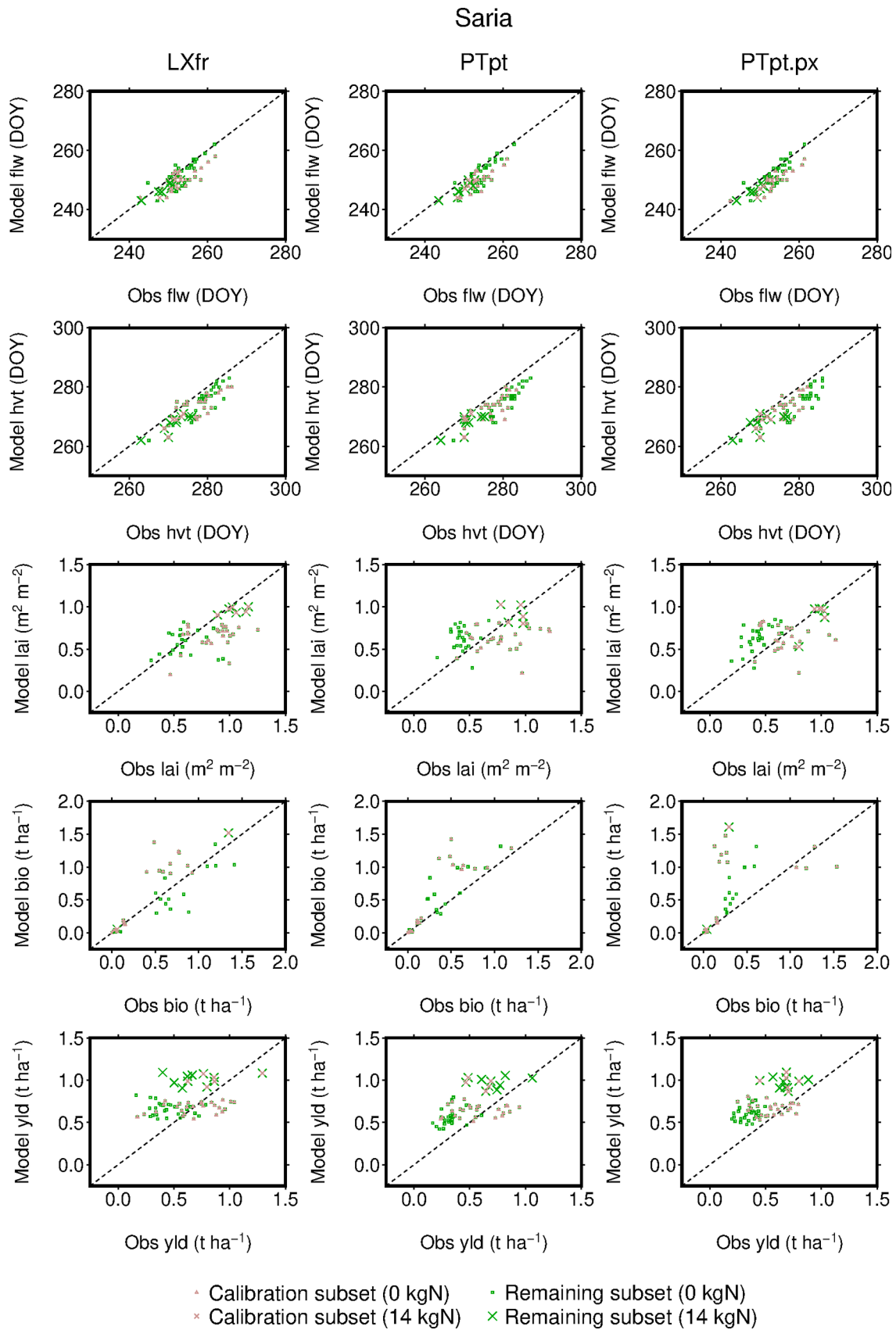


Fig. 3. Observed and modeled root-zone soil water content for each soil type in the cowpea field at Saria experimental station. The three soil types are ferric lixisols [LXfr; root-zone soil depth ( $d$ )=75 cm; plant-extractable root-zone soil water capacity ( $W_{max}$ )=169 mm  $H_2O$ ], petric plinthosols (PTpt;  $d = 50$  cm;  $W_{max}$ =83 mm  $H_2O$ ), and pisoplinthic petric plinthosols (PTpt.px;  $d = 25$  cm;  $W_{max}$ =37 mm  $H_2O$ ). DOY indicates the day of year. Simulated values using local weather observations are presented. Observed daily rainfall at the experimental station is also shown for reference.



**Fig. 4.** Observed and modeled cowpea development, growth, and yields at Saria experimental station. Dates of flowering (flw) and harvesting (hvt), as well as season maximum LAI (lai), season maximum above-ground biomass (bio; grain, stem and leaves together), and grain yield (yld) for the calibration subset only and for all data, are shown for each soil type. Data for different N application rates (0 kgN and 14 kgN) are labeled separately.

patterns of the soil types and identify the optimal season rainfall for cowpea, the rainfall was approximately 550 mm (Fig. S5 a) and wetter than the observed results (around 450 mm; Fig. 1a). For the yield response to heavy rainfall events and the number of dry days, the model captured the different response patterns between LX and PT soils qualitatively well. The JCS forcing data showed that annual precipitation was 1.5-times larger than that observed at the experimental station (Table S5). This discrepancy explains why the wet bias observed in the model-reproduced optimal rainfall.

### 3.3. Changes in rainfall patterns

Over West Africa, the frequency of heavy rainfall events during the cowpea growing season has increased in the recent past and is likely to continue to increase in the near future. The average difference in the 100-member ensemble between the d4PDF factual and non-warming counterfactual climate simulations shows a significant increase in the number of heavy rainfall days over the region under factual climate conditions in recent decades (1990–2019), compared to the preindustrial climate represented by the counterfactual simulations (Fig. 5d). On the other hand, the d4PDF simulations show a regionally contrasting change in the seasonal rainfall and the number of dry days, with dry conditions increasing in the northern parts and wet conditions increasing in the southern parts of the region (Fig. 5a, g).

The CMIP6 ensemble projections show that in the historical simulations, the spatial patterns of the changes in seasonal rainfall and the number of dry days from the preindustrial period (1850–1900) to the present (1990–2019) contrast with those of the d4PDF estimate, i.e., moisture is increasing in the northeast and decreasing in the southwest (Fig. 5g, h). The historical increase in heavy rainfall events is not significant in the CMIP6 estimate, but the d4PDF and CMIP6 estimates show an increasing trend (Fig. 5d, e). Under the CMIP6 estimates, the changes in historical rainfall patterns described above are projected to intensify in the near future (2020–2049) (Fig. 5c, f, i). While historical changes in seasonal rainfall and in the number of dry days vary depend on the sources of climate information (d4PDF and CMIP6), an increase in

heavy rainfall leading to excessive soil water is a common projected trend between these sources of climate information.

### 3.4. Projected impacts of soil water excess and deficit

Yield reductions associated with a 1-in-100 year extremely wet seasonal rainfall event would likely become more severe than they are at present, irrespective of soil type and whether the varieties used are tolerant to excessive soil water. On the other hand, reduced yields due to extreme drought events will be comparable to current droughts.

In LX soils, the effects of adopting excessive-soil-water-tolerant cowpeas in the current climate are clearly observed for the experimental station when the empirical cumulative distribution function (CDF) of the modeled yields of a tolerant variety (ID 19) is compared with the CDF of all the varieties considered in this study, except ID 19 (vertical dashed line and solid cyan line in Fig. 6f). Even with the tolerant variety, the yield in a 1-in-100 extremely wet year ( $0.091 \text{ t ha}^{-1}$ ) is projected to be as low as one-fourth of that in an extremely wet year in the present ( $0.402 \text{ t ha}^{-1}$ ) (vertical cyan line and magenta line in Fig. 6f). In tests using 1000 bootstrap replicates, the difference in the yields of the tolerant variety in future and present-day climates is significant [ $p < 0.001$ ; mean difference of  $-0.251 \text{ t ha}^{-1}$  at a 90 %-confidence interval (CI) of  $-0.356$  to  $-0.112 \text{ t ha}^{-1}$ ]. As in LX soils, similar yield results were obtained for PT soils despite their good drainage, which were  $0.417 \text{ t ha}^{-1}$  and  $0.352 \text{ t ha}^{-1}$  in the present-day and projected extremely wet years, respectively (Fig. 6g), although the yield difference is not significant ( $-0.037 \text{ t ha}^{-1}$ ; CI,  $-0.145$  to  $0.041 \text{ t ha}^{-1}$ ).

The significant increase in the average number of heavy rainfall days ( $p < 0.001$ ;  $+0.5$  days;  $+0.3$  to  $+0.7$  days) is a driver of the projected yield reductions in extremely wet years. In addition, the projected increase in seasonal rainfall ( $p < 0.001$ ;  $+25.6 \text{ mm}$ ;  $+13.0$  to  $+37.7 \text{ mm}$ ) would lead to an increase in the occurrence of seasonal rainfall that exceeds the optimal level for cowpea yields (Fig. 6a). A theoretical reduction in evapotranspiration under elevated  $[\text{CO}_2]$  is also thought to occur. These changes in combination would likely cause increases in soil water content to levels approaching saturation more frequently than in

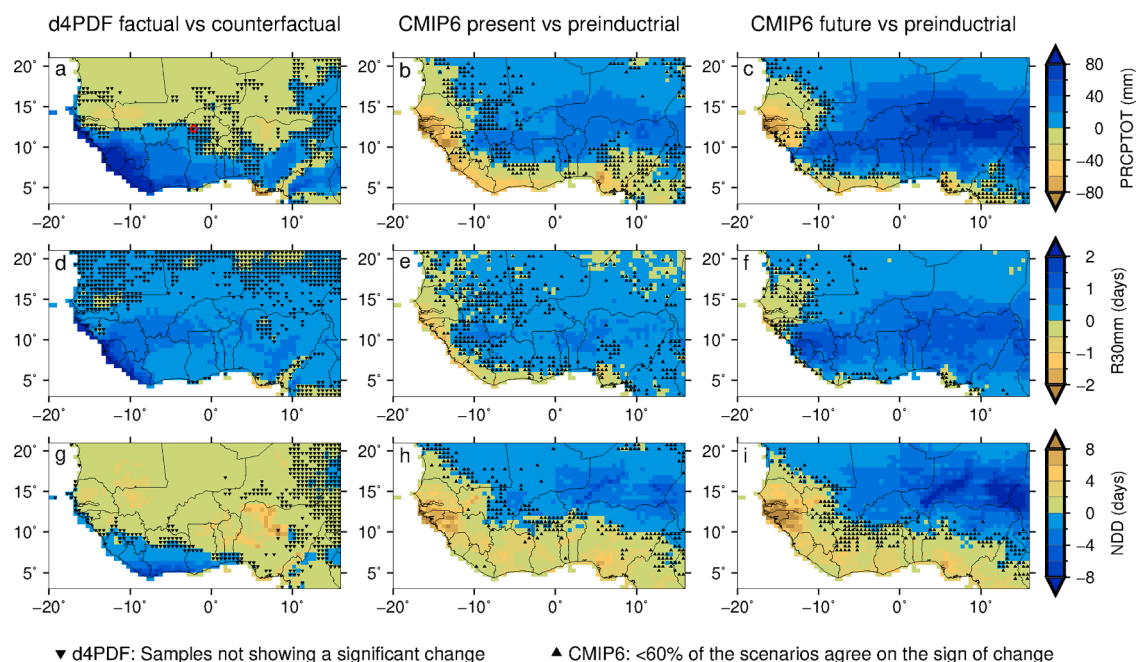


**Fig. 5.** Historical and projected changes in rainfall patterns. Displayed are cowpea-season total rainfall (a, b, c; PRCPTOT), number of heavy rainfall days (d, e, f; R30mm), and number of dry days (g, h, i; NDD) for the difference between the d4PDF factual and counterfactual simulations (1990–2019), as well as the change in the CMIP6 simulations for the present (1990–2019) and near future (2020–2049), relative to the preindustrial period (1850–1900) of historical simulations. The cowpea growing season spans approximately three months from day-of-year 200 (July 19) to 290 (October 17). The red circle in a indicates the location of Saria experimental station.

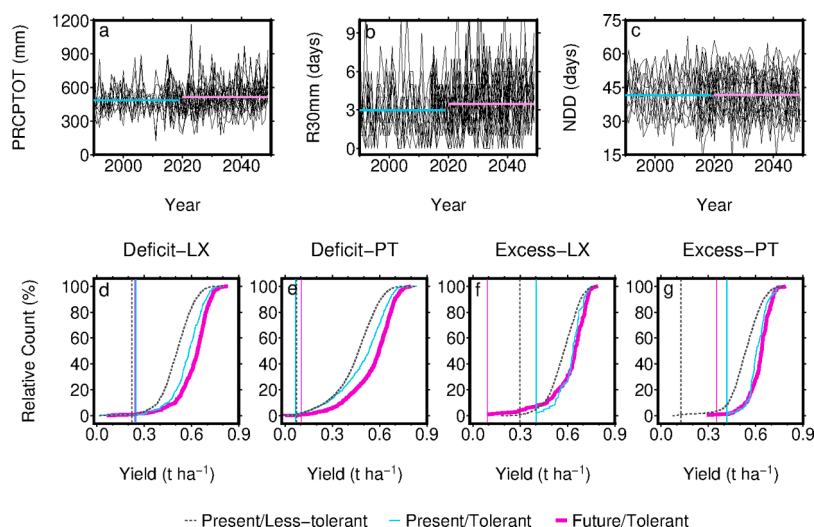


**Fig. 6.** CMIP6-projected change in rainfall patterns and yields under soil water excess and deficit. (Top row) Seasonal rainfall (a, PRCPTOT), number of heavy rainfall days (b, R30mm), and number of dry days (c, NDD) at Saria experimental station, with average rainfall for the period 1990–2019 (cyan lines) and 2020–2049 (magenta lines). (Bottom row) Empirical cumulative distribution functions (CDFs) of modeled yield with respect to varieties with and without drought- or excessive-soil-water-tolerance under present-day and near-future climates. Vertical lines indicate yield in extremely dry and wet years at a frequency of 1 in 100 years. Varieties tolerant to soil water deficit and excess are ID 12 and ID 19, respectively. Samples used to derive the CDFs consist of the radiative forcing scenarios, global climate models, bias-correction methods, varieties considered, and years.

the present-day climate.

In contrast, with current drought-tolerant varieties (ID 12), the yield in a 1-in-100 extremely dry year is projected to be as severe as current levels for both soil types ( $0.248 \text{ t ha}^{-1}$  and  $0.242 \text{ t ha}^{-1}$  for LX soils and  $0.068 \text{ t ha}^{-1}$  and  $0.103 \text{ t ha}^{-1}$  for PT soils under present-day and projected climate conditions, respectively) (Fig. 6d, e). While the yield difference is not significant for LX soils, it is significant for PT soils ( $p < 0.01$ ;  $0.045 \text{ t ha}^{-1}$ ; CI,  $0.006$  to  $0.089 \text{ t ha}^{-1}$ ). Since the projected average number of dry days shows no significant change, it is considered that the increase in water-use efficiency and  $\text{CO}_2$  fertilizer effect would offset the increased potential evapotranspiration under warmer conditions, which could worsen drought damage.

#### 4. Discussion

Yield reduction in response to excessive soil water has been observed in some agricultural environments; poorly drained soils under cooler climates (Rosenzweig et al., 2002; Li et al., 2019), over-irrigation (e.g., irrigation replenishment at 125 % of the actual evapotranspiration rate; Irmak 2014), and the cultivation of non-rice crops in paddy fields (Mitchell et al. 2013) are known examples. Although relatively few studies have examined cases in which cowpea has been planted in rice paddies, examples of other legume crops being planted in lowland paddies after rice include soybean and groundnuts in Cambodia (Mitchell et al. 2013) and soybean grown in an upland field converted from a paddy in Japan (Sugimoto et al., 1988; Bajgain et al. 2015). In addition to these cases, this study clarified the adverse effect of excessive soil water on cowpea yields, even in upland fields in the dry environments of West Africa, and how soil drainage characteristics affect yields reductions due to soil water excess.

More specifically, Iseki et al. (2021) reported that the factors affecting yield reduction in cowpea grown under excessive soil water conditions in the Sudan Savanna include low air volume and high soil temperature in the surface soil layer (0–10 cm). LX has fewer macropores ( $>75 \mu\text{m}$ ) than PT (Ikazaki et al., 2018), which means that LX has reduced drainage potential and is less aerated when heavy rainfalls occur [air volume  $<25 \%$  in LX soils; Iseki et al. (2021)] (Fig. S7). Soil temperatures at the surface layer often exceed  $35 \text{ }^\circ\text{C}$  and sometimes reach  $40 \text{ }^\circ\text{C}$  (Iseki et al., 2021), which increases soil respiration and leads to a marked decrease in the oxygen content of the soil air, which in turn

suppresses root nitrogen fixation, and consequently, limits both growth and increases in yield (Bordeleau and Prévost 1994; Maekawa et al., 2011).

There are a few limitations need to be solved for more accurate simulation. The crop model used in this study considers stress due to low aeration under soil saturation, but not soil temperature, which should be addressed in the future research. Although N fixation of cowpea is highly sensitive to soil water conditions (Hong et al., 1977), it is difficult to distinguish N deficit stress due to leaching from suppressed root nitrogen fixation, since both occur at the same time after heavy rainfall events. In addition, since the model used does not consider the lateral movement of soil water and inundation, or pests and diseases under wet conditions, these factors need to be considered to derive more plausible estimates of the impacts of soil water excess. Partly related to this, further model calibration is needed since the different levels of overestimation between the above-ground biomass and yield (RMSE of 62–185 % and 46–54 %, respectively; Table S3, Fig. 4) indicate the possibility of compensation, presumably due to the modeled abiotic stress levels being more severe than actual levels. Given that the coefficient of variation of the reported yields is 29 %, more accurate yield simulations would provide a more reliable view on the risk of soil water excess in a changing climate.

Our findings indicate that droughts will remain a major climate hazard, while heavy rainfall events will emerge as an alarming, relatively serious threat to food security and nutrition in West African in the coming decades. The projected increase in heavy rainfall events will be a consistent direction of change, even if the direction of projected changes in seasonal rainfall is uncertain (Dosio et al., 2020). Cowpea is not only a source of protein, but also a source of income that is used to compensate for the lack of home-produced staple grains (Shiratori et al., 2020).

Countermeasures similar to those that have been employed for drought risk reduction need to be developed for excessive soil water, as doing so will safeguard small-scale farmer incomes, and ultimately, food security and nutrition in West Africa. Possible solutions include the development of crop recommendation guidelines based on soil type, or more simply, based on the distance from the main river channel. Such guidelines would support farmers to selectively grow crops that are more tolerant to excessive soil water than cowpeas in poorly drained fields. To this end, soil classification services that are affordable to small-scale farmers are valuable. In parallel, cataloging crop tolerance to



excessive soil water is encouraged, possibly using an approach that is analogous to the crop water requirements of Brouwer and Heibloem (1986) that guides farmers in selecting which crops could be grown based on water availability and drought risk.

### Author contributions

T.I. has conceptualized, developed methodology, and conducted formal analysis; K.Iseki, K.Ikazaki, and T.S. have contributed to conceptualization and handled project administration; H.S. and Y.I. have curated climate data and helped investigation; K.Iseki, K.Ikazaki, T.S., and B.J.B. have curated crop data and helped investigation; all authors have contributed to writing the original draft, review, and editing.

### Declaration of Competing Interest

The authors declare that they have no known competing financial interests or personal relationships that could have appeared to influence the work reported in this paper.

### Data availability

Data will be made available on request.

### Acknowledgments

We thank Martin Sanon, Emmanuel Sanon, and Jpsaphat Sanon at Agro-Action for their support with field management and data collection; the High-Performance Cluster Computing System at the Agriculture, Forestry and Fisheries Research Information Technology Center for support with the crop model simulations; and the World Climate Research Programme, which, through its Working Group on Coupled Modelling, coordinated and promoted CMIP6. The climate modeling groups are thanked for producing and making their model outputs available; the Earth System Grid Federation (ESGF) for archiving the data and providing access; and the multiple funding agencies who support CMIP6 and ESGF. This study was conducted as part of international collaborative research projects between JIRCAS and INERA (“Development of soil and crop management technologies to stabilize upland farming systems of African smallholder farmers”) that were funded by the Ministry of Agriculture, Forestry and Fisheries, Japan. TI was partly supported by the Environment Research and Technology Development Fund (JPMEERF20202002 and JPMEERF23S21120) of the Environmental Restoration and Conservation Agency Provided by the Ministry of the Environment; and by Grants-in-Aid for Scientific Research (22H00577 and 20K06267) from the Japan Society for the Promotion of Science. YI and HS were supported by the Advanced Studies of Climate Change Projection (SENTAN, JPMXD0722680395) of the Ministry of Education, Culture, Sports, Science and Technology of Japan.

### Supplementary materials

Supplementary material associated with this article can be found, in the online version, at [doi:10.1016/j.agrformet.2023.109783](https://doi.org/10.1016/j.agrformet.2023.109783).

### References

- Anderson, W., et al., 2021. Violent conflict exacerbated drought-related food insecurity between 2009 and 2019 in sub-Saharan Africa. *Nat. Food* 2, 603–615.
- Arias, P.A., et al., 2021. Technical summary. In: Masson-Delmotte, V., et al. (Eds.), *Climate Change 2021: The Physical Science Basis*. Cambridge University Press, pp. 33–144.

- Bajgain, R., et al., 2015. Biomass production and yield of soybean grown under converted paddy fields with excess water during the early growth stage. *Field Crops Res.* 180, 221–227.
- Bastos, E.A., et al., 2011. Identification of cowpea genotypes for drought tolerance. *Rev. Ciên. Agron.* 42, 100–107.
- Bordeleau, L.M., Prévost, D., 1994. Nodulation and nitrogen fixation in extreme environments. *Plant Soil* 161, 115–125.
- Brouwer, C., Heibloem, M., 1986. Chapter 3 crop water needs. *Irrigation Water Management Training Manual No. 3*. FAO.
- Brown, M.E., Pinzon, J.E., Prince, S.D., 2006. The effect of vegetation productivity on millet prices in the informal markets of Mali, Burkina Faso and Niger. *Clim. Change* 78, 181–202.
- Callo-Concha, D., et al., 2013. Farming in the West African Sudan Savanna: insights in the context of climate change. *Afr. J. Agric. Res.* 8, 4693–4705.
- Carrão, H., Naumann, G., Barbosa, P., 2016. Mapping global patterns of drought risk: an empirical framework based on sub-national estimates of hazard, exposure and vulnerability. *Glob. Environ. Change* 39, 108–124.
- Cleveland, W.S., 1979. Robust locally weighted regression and smoothing scatterplots. *J. Amer. Statist. Assoc.* 74, 829–836.
- Craufurd, P.Q., Subedi, M., Summerfield, R.J., 1997. Leaf appearance in cowpea: effects of temperature and photoperiod. *Crop Sci.* 37, 167–171.
- Donat, M., et al., 2016. More extreme precipitation in the world’s dry and wet regions. *Nat. Clim. Change* 6, 508–513.
- Dosio, A., et al., 2020. A tale of two futures: contrasting scenarios of future precipitation for West Africa from an ensemble of regional climate models. *Environ. Res. Lett.* 15, 064007.
- Food and Agriculture Organization (FAO), 2022. FAOSTAT. <https://nam11.safelinks.protection.outlook.com/?url=https%3A%2F%2Fwww.fao.org%2Ffaostat%2Fen%2F%23data&data=05%7C01%7C7c.panneerselvam%40elsevier.com%7Cce1a231f88b940e83c0c08dbd6d73d85%7C9274ee3f94254109a27f9fb15c10675d%7C0%7C0%7C638339992176981443%7CUnknown%7CTWFPbGZsb3d8eyJWJjoIMC4wLjAwMDAilCJQJoiV2luMzIlLk1haWwLlCJXVCi6Mn0%3D%7C3000%7C%7C%7C&sdata=Vmq9hpXeQCEbnq5zWUYQ3WSXqufOyXr8bkq9525gwk%3D&reserved=0>.
- Food and Agriculture Organization, 2021. The impact of disasters and crises on agriculture and food security: 2021. FAO, Rome. <https://doi.org/10.4060/cb3673en>.
- Hong, T.D., Minchin, F.R., Summerfield, R.J., 1977. Recovery of nodulated cowpea plants (*Vigna unguiculata* (L.) Walp.) from waterlogging during vegetative growth. *Plant Soil* 48, 661–672.
- Huang, J., van den Dool, H.M., Georganakos, K.P., 1996. Analysis of model-calculated soil moisture over the United States (1931–1993) and applications to long-range temperature forecasts. *J. Clim.* 9, 1350–1362.
- Iizumi, T., et al., 2017. Responses of crop yield growth to global temperature and socioeconomic changes. *Sci. Rep.* 7, 7800.
- Iizumi, T., et al., 2018. Crop production losses associated with anthropogenic climate change for 1981–2010 compared with preindustrial levels. *Int. J. Climatol.* 38, 5405–5417.
- Iizumi, T., et al., 2021a. Rising temperatures and increasing demand challenge wheat supply in Sudan. *Nat. Food* 2, 19–27.
- Iizumi, T., et al., 2021b. Aligning the harvesting year in global gridded crop model simulations with that in census reports is pivotal to national-level model performance evaluations for rice. *Euro. J. Agron.* 130, 126367.
- Ikazaki, K., Nagumo, F., Simporé, S., Barro, A., 2018. Soil toposequence, productivity, and a simple technique to detect petroplinthites using ground-penetrating radar in the Sudan Savanna. *Soil Sci. Plant Nutr.* 64, 623–631.
- Irmak, S., 2014. Plant Growth and Yield as Affected by Wet Soil Conditions Due to Flooding or Over-Irrigation. Nebraska Extension Publications, p. G1904. <https://extensionpubs.unl.edu/publication/9000016366481/plant-growth-and-yield-as-affected-by-wet-soil-conditions-due-to-flooding-or-over-irrigation/>.
- Iseki, K., Ikazaki, K., Batiemo, J.B., 2021. Cowpea yield variation in three dominant soil types in the Sudan Savanna of West Africa. *Field Crops Res.* 261, 108012.
- Iseki, K., Ikazaki, K., Batiemo, B.J., 2023. Heterogeneity effects of plant density and fertilizer application on cowpea grain yield in soil types with different physicochemical characteristics. *Field Crops Res.* 292, 108825.
- Ishikawa, S., Nakashima, T., Iizumi, T., Hare, M.C., 2021. Evaluating irrigated rice yields in Japan within the Climate Zonation Scheme of the Global Yield Gap Atlas. *J. Agric. Sci.* 158, 718–729.
- Jägermeyr, J., et al., 2021. Climate impacts on global agriculture emerge earlier in new generation of climate and crop models. *Nat. Food* 2, 873–885.
- Kim, W., Iizumi, T., Nishimori, M., 2019. Global patterns of crop production losses associated with droughts from 1983 to 2009. *J. Appl. Meteorol. Climatol.* 58, 1233–1244.
- Kim W., Iizumi T., Hosokawa N., Tanoue M., Hirabayashi Y., 2023. Flood impacts on global crop production: advances and limitations. *Environ. Res. Lett.* 18, 054007.
- Li, Y., Guan, K., Schnitkey, G.D., DeLucia, E., Peng, B., 2019. Excessive rainfall leads to maize yield loss of a comparable magnitude to extreme drought in the United States. *Glob. Change Biol.* 25, 2325–2337.
- Maekawa, T., Shimamura, S., Shimada, S., 2011. Effects of short-term waterlogging on soybean nodule nitrogen fixation at different soil reductions and temperatures. *Plant Prod. Sci.* 14, 349–358.
- Mitchell, J., et al., 2013. Wet cultivation in lowland rice causing excess water problems for the subsequent non-rice crops in the Mekong region. *Field Crops Res.* 152, 57–64.
- National Academies of Sciences, Engineering, and Medicine, 2005. *Dietary Reference Intakes for Energy, Carbohydrate, Fiber, Fat, Fatty Acids, Cholesterol, Protein, and*

- Amino Acids. The National Academies Press, Washington, DC. <https://doi.org/10.17226/10490>.
- Neitsch, S.L., Arnold, J.G., Kiniry, J.R., Williams, J.R., 2005. Soil and Water Assessment Tool Theoretical Documentation (Version 2005). USDA.
- Padi, F.K., Ehlers, J.D., 2008. Effectiveness of early generation selection in cowpea for grain yield and agronomic characteristics in semiarid West Africa. *Crop Sci.* 48, 533–540.
- Padi, F., 2004. Relationship between stress tolerance and grain yield stability in cowpea. *J. Agric. Sci.* 142, 431–443.
- R Core Team, 2021. R: A language and Environment for Statistical Computing. R Foundation for Statistical Computing, Vienna, Austria.
- Rosenzweig, C., Tubiello, F.N., Goldberg, R., Mills, E., Bloomfield, J., 2002. Increased crop damage in the US from excess precipitation under climate change. *Glob. Environ. Change* 12, 197–202.
- Samberg, L.H., Gerber, J.S., Ramankutty, N., Herrero, M., West, P.C., 2016. Subnational distribution of average farm size and smallholder contributions to global food production. *Environ. Res. Lett.* 11, 124010.
- Sanginga, N., Lyasse, O., Singh, B., 2000. Phosphorus use efficiency and nitrogen balance of cowpea breeding lines in a low P soil of the derived savanna zone in West Africa. *Plant Soil* 220, 119–128.
- Shiratori, S., Sawadogo-Compaore, E.M.F.W., Chien, H., 2020. Variation of cowpea production and usage in rural households: a comparison between northern and southern Burkina Faso. *Jpn. Agric. Res. Q.* 54, 263–270.
- Smale, M., Thériault, V., 2021. Input subsidy effects on crops grown by smallholder farm women: the example of cowpea in Mali. *Oxford Dev. Stud.* <https://doi.org/10.1080/13600818.2021.2008892>.
- Sousa, D., et al., 2018. Radiation use efficiency for cowpea subjected to different irrigation depths under the climatic conditions of the northeast of Pará State. *Rev. Bras. Meteorol.* 33, 579–587.
- Sugimoto, H., Amemiya, A., Satou, T., Takenouchi, A., 1988. Excess moisture injury of soybeans cultivated in a upland field converted from paddy: I. Effects of excessive soil moisture on dry matter production and seed yield. *Jpn. J. Crop Sci.* 57, 71–76.
- Sultan, B., DeFrance, D., Iizumi, T., 2019. Evidence of crop production losses in West Africa due to historical global warming in two crop models. *Sci. Rep.* 9, 12834.
- United Nations. **World population prospects 2022**. <https://population.un.org/wpp/Download/Standard/MostUsed/>.
- Urban, D.W., et al., 2015. The effects of extremely wet planting conditions on maize and soybean yields. *Clim. Change* 130, 247–260.
- van Heerwaarden, J., et al., 2023. Consistency, variability, and predictability of on-farm nutrient responses in four grain legumes across East and West Africa. *Field Crops Res.* 299, 108975.
- Vasconcelos, I.M., et al., 2010. Protein fractions, amino acid composition and antinutritional constituents of high-yielding cowpea cultivars. *J. Food Compos. Anal.* 23, 54–60.
- Vogel, E., et al., 2019. The effects of climate extremes on global agricultural yields. *Environ. Res. Lett.* 14, 054010.
- Wang, R., Bowling, L.C., Cherkauer, K.A., 2016. Estimation of the effects of climate variability on crop yield in the Midwest USA. *Agric. For. Meteorol.* 216, 141–156.